International Journal of Innovative Computing, Information and Control
Volume **21**, Number **1**, February **2025**

 ISSN 1349-4198
pp. **239–250**

IMAGE RECONSTRUCTION FROM INCOMPLETE SAMPLE USING TOTAL VARIATION AND MAGNITUDE DIFFERENCE AVERAGING

Ratri Dwi Atmaja[1] and Sugondo Hadiyoso[2]

[1]School of Electrical Engineering
[2]School of Applied Science
Telkom University
Jl. Telekomunikasi No. 1, Terusan Buah Batu, Bandung 40257, Indonesia
{ ratridwiatmaja; sugondo }@telkomuniversity.ac.id

Received March 2024; revised July 2024

Abstract. *Many measurement cases use a limited number of sensors to estimate an original signal. It causes incomplete samples that make the estimated signal degraded. Therefore, it needs a signal processing method to improve the quality of the estimated signal. We proposed magnitude difference averaging, which aims to improve total variation (TV) performance in reconstructing an image from an incomplete frequency sample. In our experiments, this TV can clear the object structure visually but still has noise. After combining with our proposed magnitude difference averaging, 85.71% of TV results show better performance in object structure or noise conditions.*
Keywords: Image reconstruction, Incomplete frequency, Total variation, Magnitude difference averaging

1. **Introduction.** Measurement applications have the purpose of capturing objects that are not directly visible. It works by putting in some sensors to receive signals from the objects. The image quality depends on the number of sensors and noise that interfere with the signals. Using many sensors may take an expensive budget. This reason causes some measurement cases with a limited number of sensors. As a result, it works using a few sampling points and gets the image quality degraded. Therefore, we need a signal processing method to increase the image quality.

The degraded quality of imaging because of the limited sampling points is popularly known as an inverse problem. First-order total variation (TV) in [1] offers a solution to answer this inverse problem. However, it has drawbacks in the form of noise in the reconstruction result, named as staircasing effect [2]. Some researchers [3-6] present high-order TV to overcome the noise. However, high-order TV has a disadvantage in its ability to solve jump discontinuities [2]. Speckle artifacts appear when dealing with high-order TV regularizers [7].

This paper demonstrates an image reconstruction using first-order TV to finish an incomplete frequency sample. We contribute by proposing magnitude difference averaging to reduce some noise, although it increases the cost of time. In addition, we also find that the proposed method yields benefits to sharpen the object structure. This article's layout is as follows. We present the TV and the proposed magnitude difference averaging in Section 2. Next, we discuss the yields of the proposed combination method compared to TV alone in Section 3. Last, in Section 4, we give the conclusions.

DOI: 10.24507/ijicic.21.01.239

2. **Research Method.** Our proposed method in Figure 1 consists of a learning and a testing process. The learning process aims to save the magnitude difference averaging of some learning images. Meanwhile, the testing process aims to estimate a reconstruction result from a testing image. The bold arrow indicates the relationship between the two processes. The magnitude difference averaging obtained from the learning process is needed when we want to reconstruct an image in the testing process.

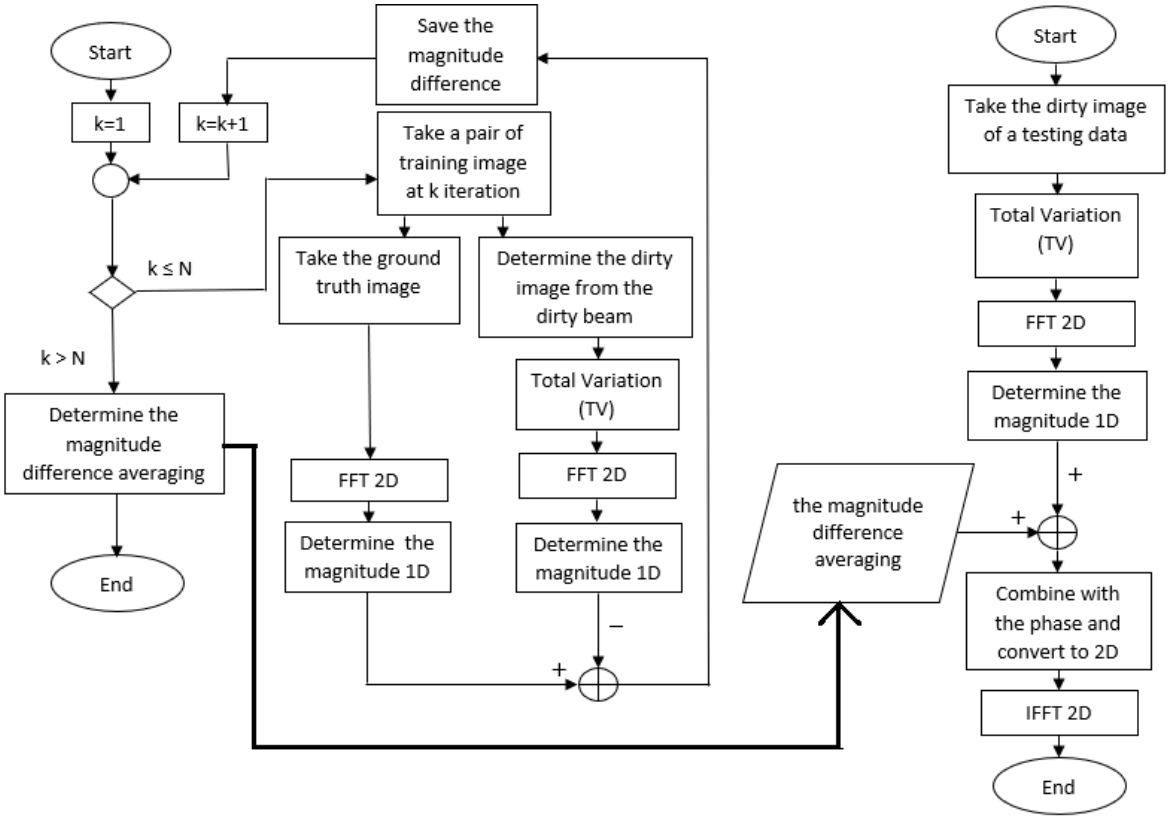

FIGURE 1. Learning process (left) and testing process (right)

In the left side of Figure 1, the learning process is repeated iteratively as N learning images. A pair of learning images consists of a ground truth image and its dirty beam. The dirty beam role is as its measurement results in incomplete frequency. We determine its dirty image using a 2D inverse fast Fourier transform directly from its dirty beam. We then use total variation (TV) to improve the dirty image. This TV method needs input from the dirty image of a ground truth image. As stated in [1], we can define the TV of d:

$$\|d\|_{TV} = \sum_k \sum_l \sqrt{|d_{k+1,l} - d_{kl}|^2 + |d_{k,l+1} - d_{kl}|^2}. \tag{1}$$

We have an image d with the size of $n \times n$ and d_{kl} as pixels in coordinate (k, l). Or we can write these three operators:

$$P_{h;kl}d = \begin{cases} d_{k+1,l} - d_{kl}, & k < n \\ 0 & k = n \end{cases}, \tag{2}$$

$$P_{v;kl}d = \begin{cases} d_{k,l+1} - d_{kl}, & l < n \\ 0 & l = n \end{cases}, \tag{3}$$

and

$$P_{kl}d = \left(\frac{P_{h;kl}d}{P_{v;kl}d} \right), \tag{4}$$

then the TV of d is

$$\|d\|_{TV} = \sum_{kl} \sqrt{(P_{h;kl}d)^2 + (P_{v;kl}d)^2} = \sum_{kl} \|P_{kl}d\|_2. \tag{5}$$

We can use TV regularization with equality constraints [8] to find the recovered image:

$$\min TV(d) \text{ subject to } Ad = c. \tag{6}$$

We have a measurement matrix A and observation result c. In this learning process, we take two important 1D magnitude values. The first and second are from 2D fast Fourier transform results of the ground truth and the TV image, respectively. We then subtract the magnitude of the ground truth image from the magnitude of the TV image to obtain a magnitude difference from a pair of learning images. When looping is finished for N learning images, we save the magnitude difference averaging from N learning images.

On the right side of Figure 1, the testing process consists of some steps. First, we take a dirty image of the testing data. Second, we improve the dirty image using TV. Third, we perform a 2D fast Fourier transform to the output of the TV. Fourth, we arrange to 1D and separate the magnitude and the phase. Fifth, we sum the magnitude with the magnitude difference averaging results from the learning process. Sixth, we give back the phase to the new magnitude and arrange it to 2D. Seventh, we perform a 2D inverse fast Fourier transform to get the reconstruction result.

3. **Results and Analysis.** The first step in the experimental setup is how to generate the measurement of the ground truth image both in the learning and testing processes. This measurement indicates a process to get the incomplete sample in the frequency domain. We name the incomplete sampling result as the dirty beam. We use a binary image in the first column of Figure 2 for getting the dirty beam. Black colors indicate the positions in which we take the samples.

We use five grayscale data from [9] with the image size of 70×70 in the learning process. One data consists of a pair of images: the ground truth image and the corresponding total variation (TV) image. Figure 2 shows it from columns two and three. The left panel shows the ground truth image. Meanwhile, the right panel shows the corresponding TV image. Our idea comes from observing a pair of images in the frequency domain between the ground truth image and the corresponding TV image, especially observing the magnitude value. We find a similar pattern of magnitude difference among five pairs of images in the learning data. We show the pattern of the magnitude difference of data one to five in Figure 3. Therefore, according to the similar pattern, in the testing process, we can use the magnitude difference averaging of five learning data as the key to reconstruct a dirty image, obtaining the estimated reconstruction result.

In the testing process, we used 28 grayscale data with the image size of 70×70 also from [9] to reconstruct the dirty images. Note that these 33 data for learning and testing are ground truth images and can be downloaded directly in [9]. They are quasar images, the center of active galaxies in astronomy. We then measure it in the experimental setup to get the dirty beam. We perform a 2D inverse Fourier transform to get the dirty image. The dirty image is the input in the testing before applying TV and the magnitude difference averaging. Evaluating the quality of the reconstruction result to the ground truth image, we use the structural similarity (SSIM) index as follows [11]:

$$SSIM(x, y) = \frac{(2\mu_x\mu_y + C_1)(2\sigma_{xy} + C_2)}{(\mu_x^2 + \mu_y^2 + C_1)(\sigma_x^2 + \sigma_y^2 + C_2)}, \tag{7}$$

where x is the reconstruction result, and y is the ground truth image. In this equation, we have the mean of image intensity

$$\mu_x = \frac{1}{M}\sum_{i=1}^{M} x_i, \tag{8}$$

the standard deviation

$$\sigma_x = \left(\frac{1}{M-1}\sum_{i=1}^{M}\left(x_i - \mu_x\right)^2\right)^{1/2}, \tag{9}$$

and the cross covariance

$$\sigma_{xy} = \frac{1}{M-1}\sum_{i=1}^{M}\left(x_i - \mu_x\right)\left(y_i - \mu_y\right). \tag{10}$$

The value of C_1 and C_2 are small enough. Higher SSIM shows better results.

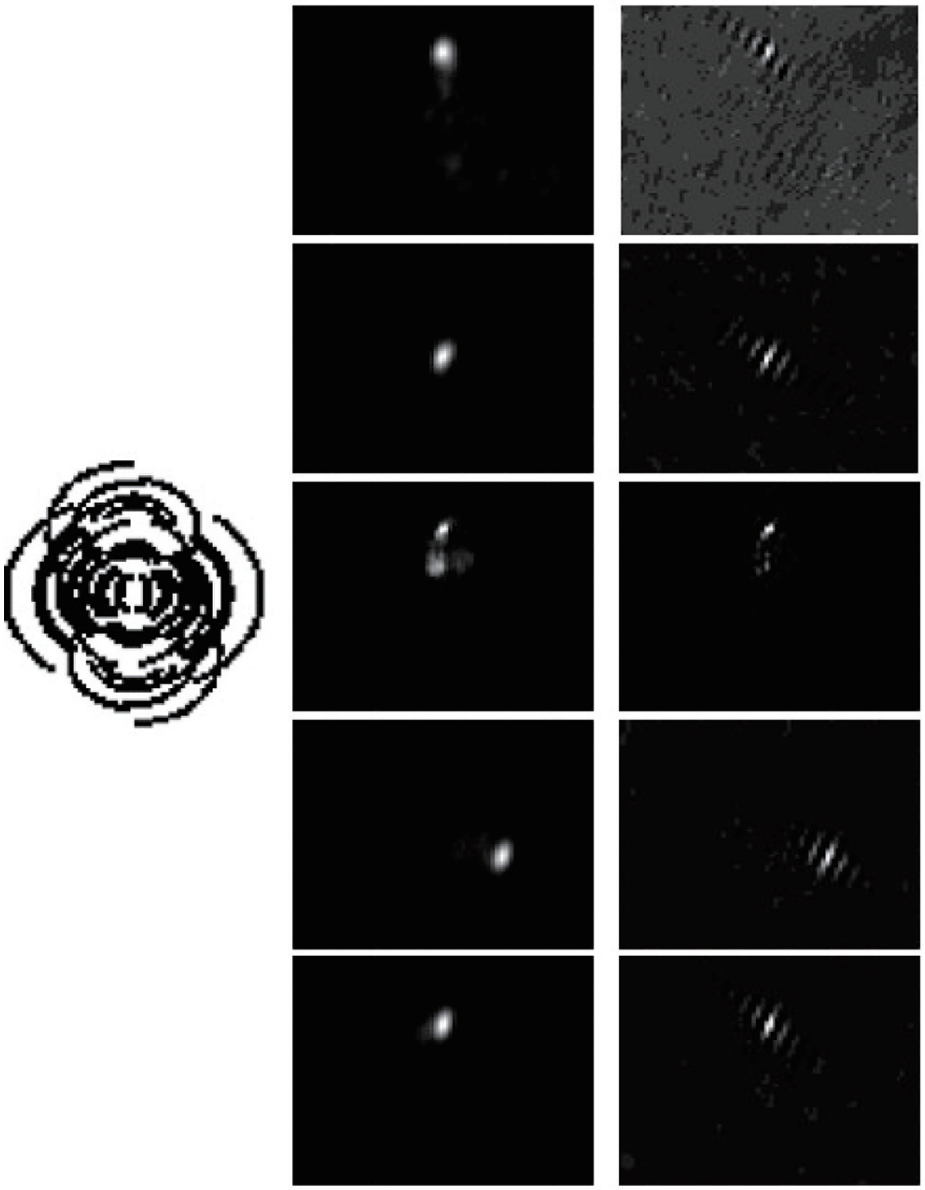

FIGURE 2. The first column shows the sampling pattern to measure the ground truth image, modified from [10]. The second and third columns show our learning images. The second column is ground truth images while the third column is the corresponding TV images.

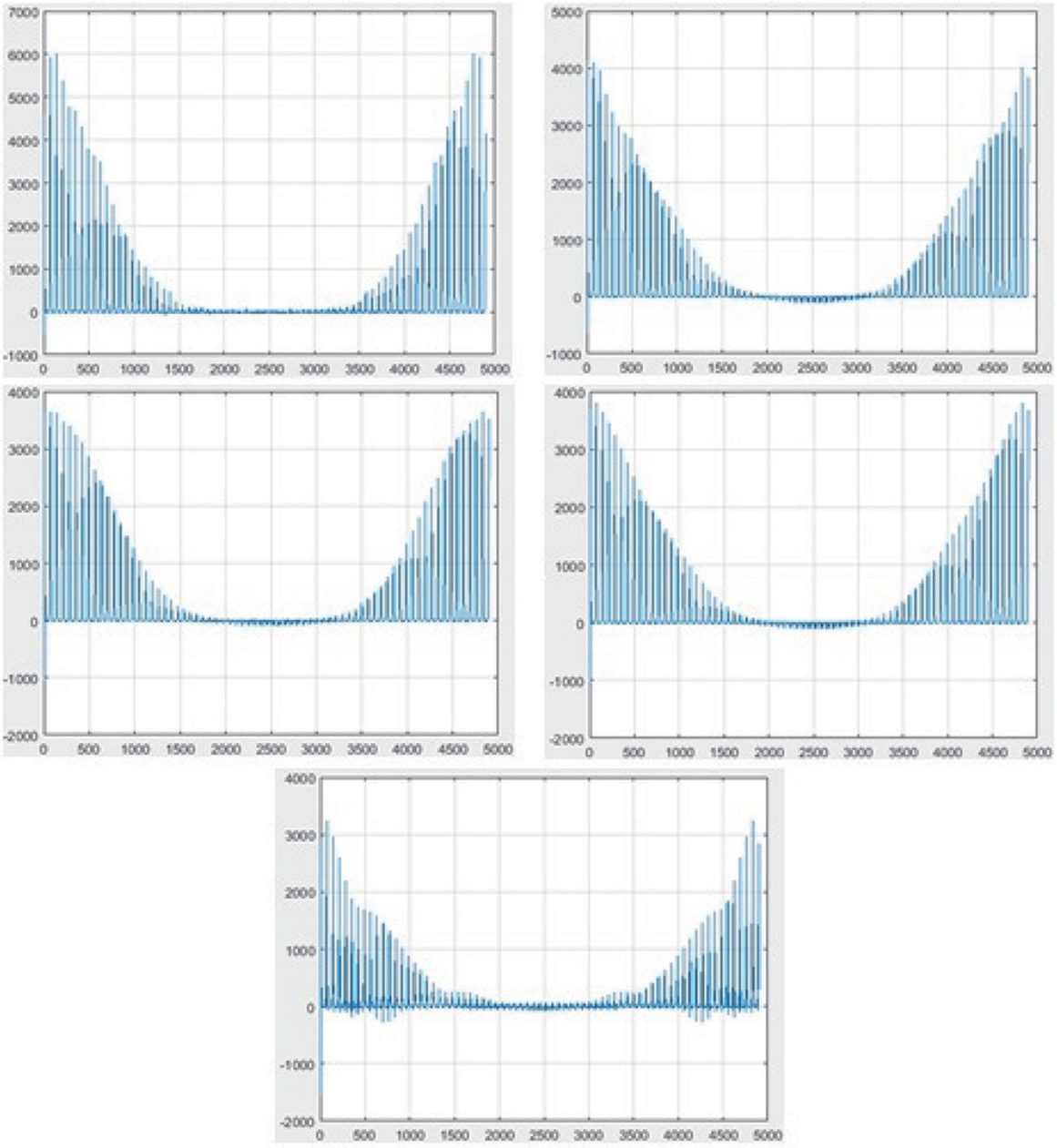

FIGURE 3. Pattern of magnitude difference in five learning data. The first row shows the magnitude difference from data one and two. The second row shows the magnitude difference from data three and four. The last row shows the magnitude difference from data five. The x-axis indicates the sample or pixel, while the y-axis indicates the magnitude value.

We present SSIM results from 28 data of testing in Table 1. We have the reconstruction results of using TV as the baseline method. Meanwhile, in the combination of TV and magnitude difference averaging, we use three, four, and five learning data to know whether more learning data can give better results. We find that 12 of 28 (42.86%) data did not have higher SSIM in more learning data. They are data of testing 4, 5, 6, 11, 12, 13, 14, 16, 19, 21, 24, and 26. They have fluctuating SSIM when using three, four, and five learning data, although the difference is small enough. There is a decline in SSIM result after adding training image when its magnitude difference made the averaging keep away from the magnitude difference of the ground truth image.

TABLE 1. SSIM results

Data of testing	SSIM TV	SSIM TV + magnitude difference averaging		
		Three learning images	Four learning images	Five learning images
1	0.8599	0.9363	0.9409	**0.9428**
2	**0.9810**	0.9699	0.9728	0.9752
3	0.8639	0.9146	0.9159	**0.9185**
4	**0.8095**	0.6887	0.6843	0.6824
5	0.8487	**0.8639**	0.8634	**0.8639**
6	0.7743	0.7963	0.7954	**0.7971**
7	0.8538	0.9609	0.9654	**0.9696**
8	**0.8926**	0.8560	0.8587	0.8606
9	0.5758	0.6793	0.6796	**0.6800**
10	0.8482	0.9703	0.9726	**0.9752**
11	0.8385	0.8619	0.8612	**0.8640**
12	**0.7826**	0.5361	0.5280	0.5258
13	**0.8113**	0.6708	0.6663	0.6659
14	**0.7272**	0.5455	0.5375	0.5343
15	0.8583	0.9152	0.9168	**0.9198**
16	**0.8608**	0.7751	0.7742	0.7741
17	0.8621	0.9309	0.9309	**0.9322**
18	0.8552	0.9666	0.9702	**0.9736**
19	**0.6905**	0.5512	0.5483	0.5492
20	0.8490	0.9475	0.9527	**0.9564**
21	**0.9037**	0.8272	0.8235	0.8224
22	0.8479	0.9514	0.9564	**0.9596**
23	0.8582	0.9270	0.9317	**0.9350**
24	**0.7137**	0.6697	0.6658	0.6657
25	0.8437	0.9397	0.9450	**0.9491**
26	0.8476	0.9265	0.9263	**0.9279**
27	0.8427	0.8936	0.8949	**0.8971**
28	0.8410	0.9371	0.9432	**0.9467**

Presented in Table 1, we observe the SSIM results from a combination of TV and magnitude difference averaging, compared to TV alone. We have 10 of 28 (35.71%) data that give lower SSIM than TV. They are data of testing 2, 4, 8, 12, 13, 14, 16, 19, 21, and 24. We then present the visual results in Figures 4-8 to see the difference between both methods in terms of object structure and noise. We categorize three groups of results: First, compared to TV, the proposed method made the data of testing 2 and 8 cleaner in noise, but it gave a bigger size in the object structure. Second, the data of testing 4, 12, 13, 16, 19, and 24 has a better object structure, but it still has noise. Third, the data of testing 14 and 21 give almost the same results in object structure and have noise. Among these three groups, visually, we observe that the proposed method can give better results than TV only in the second group, although the SSIM is lower. Meanwhile, observing the other data of testing that get higher SSIM, we have 18 of 28 (64.29%) data that give better results in object structure than TV. Moreover, some can yield lower noise. Finally, taking from these 18 objects and the second group, the proposed method can give better results on 24 of 28 data (85.71%).

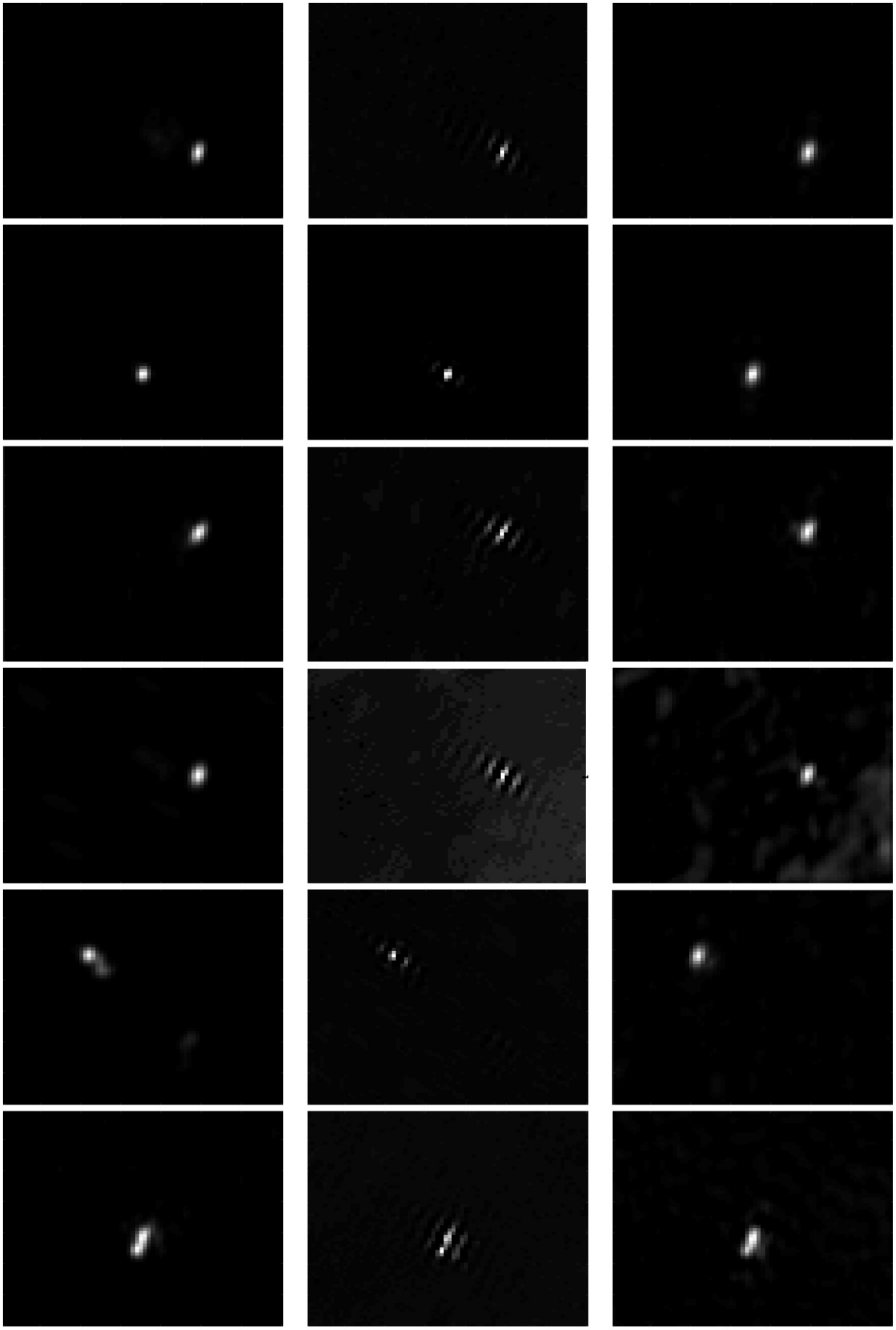

FIGURE 4. Reconstruction results of data 1 to 6. Left to right: ground truth image, TV, and proposed.

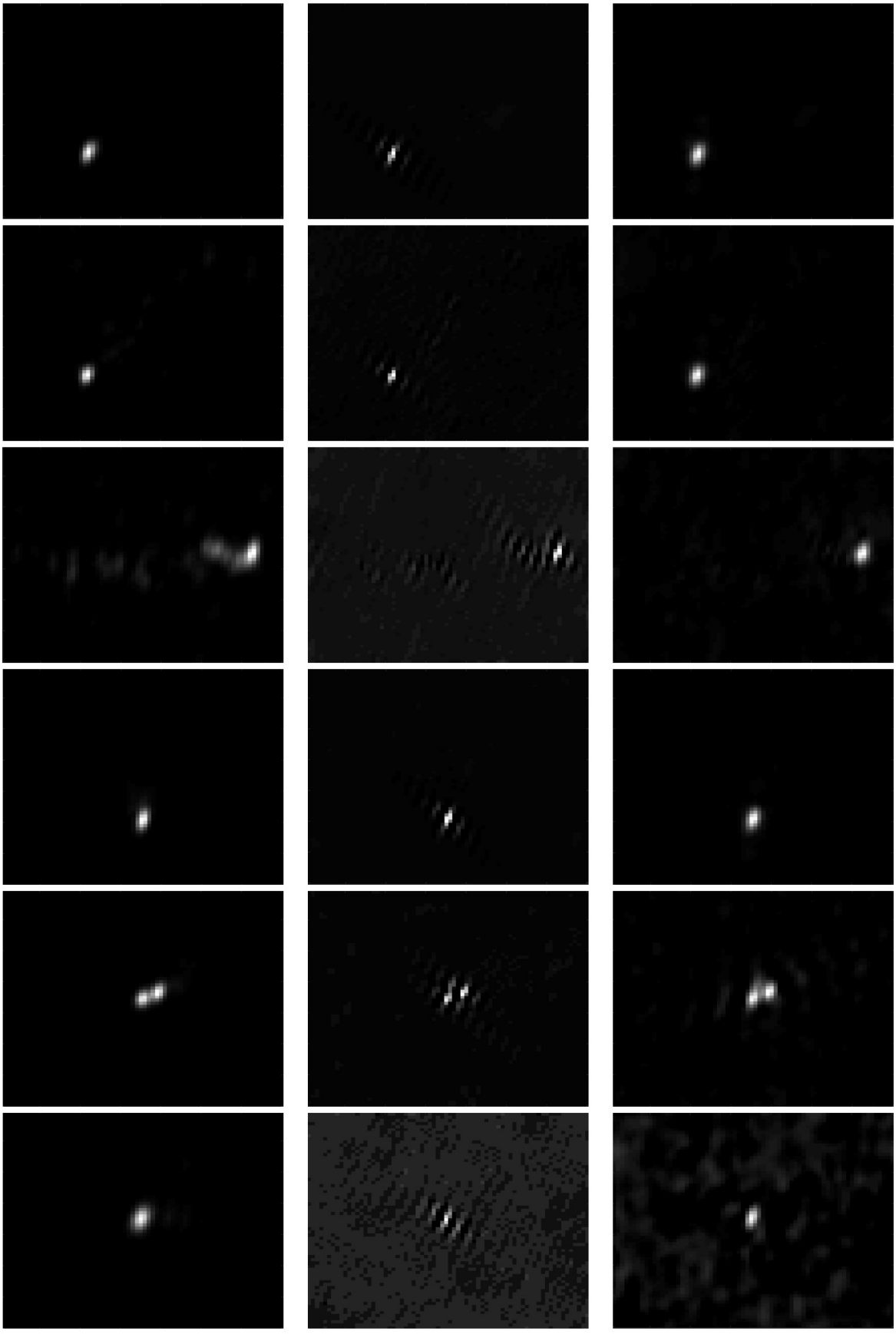

FIGURE 5. Continued reconstruction results of data 7 to 12. Left to right: ground truth image, TV, and proposed.

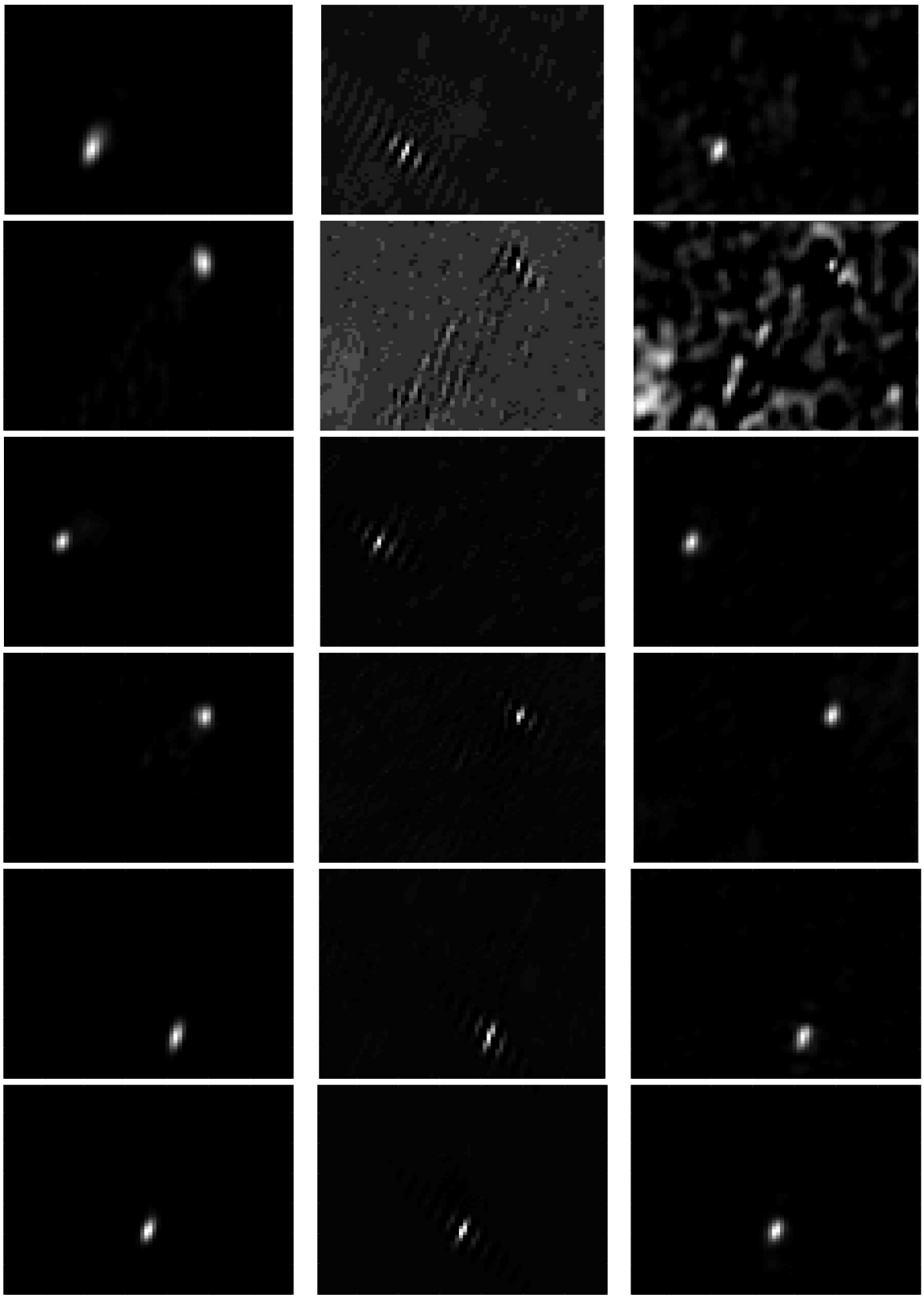

FIGURE 6. Continued reconstruction results of data 13 to 18. Left to right: ground truth image, TV, and proposed.

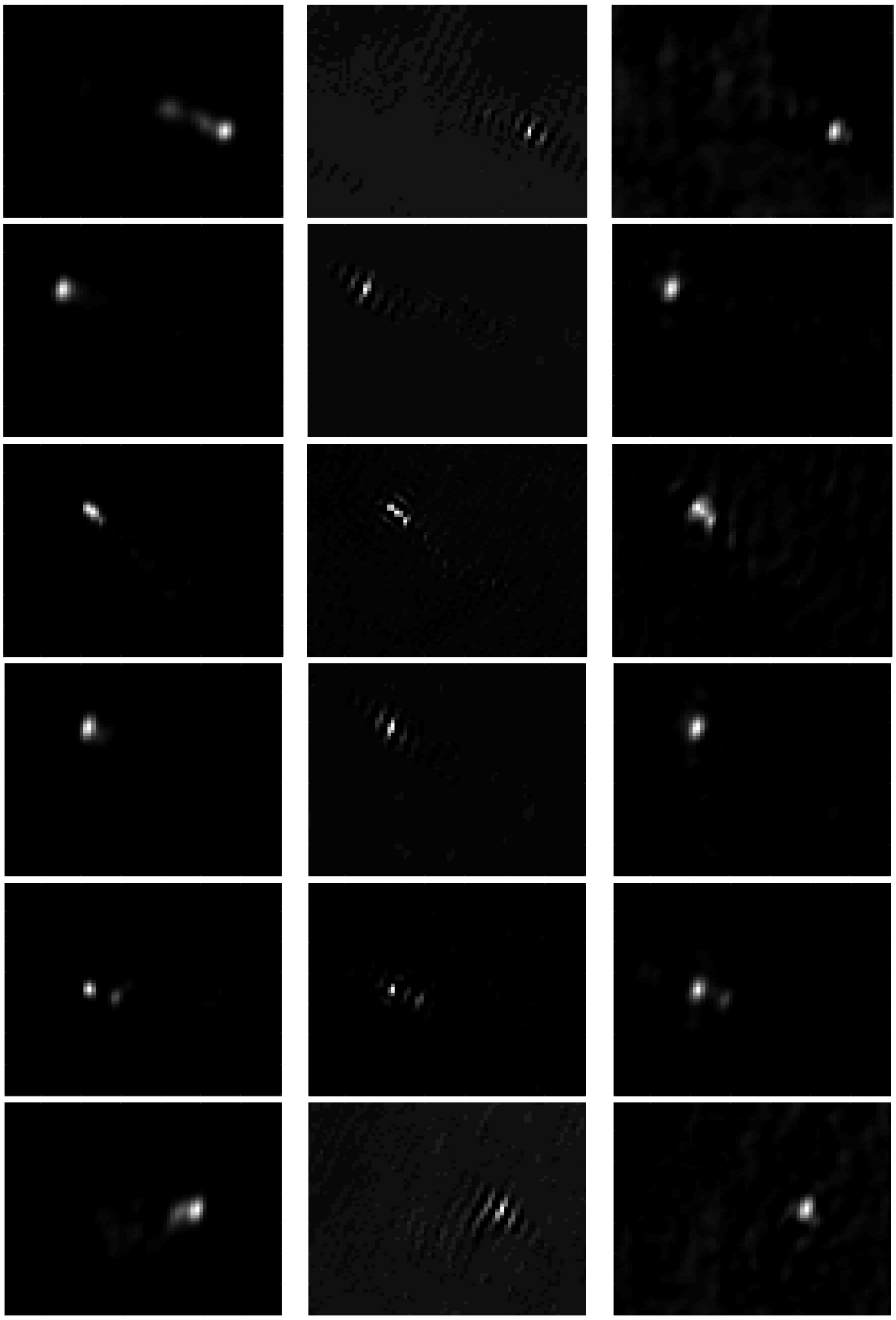

FIGURE 7. Continued reconstruction results of data 19 to 24. Left to right: ground truth image, TV, and proposed.

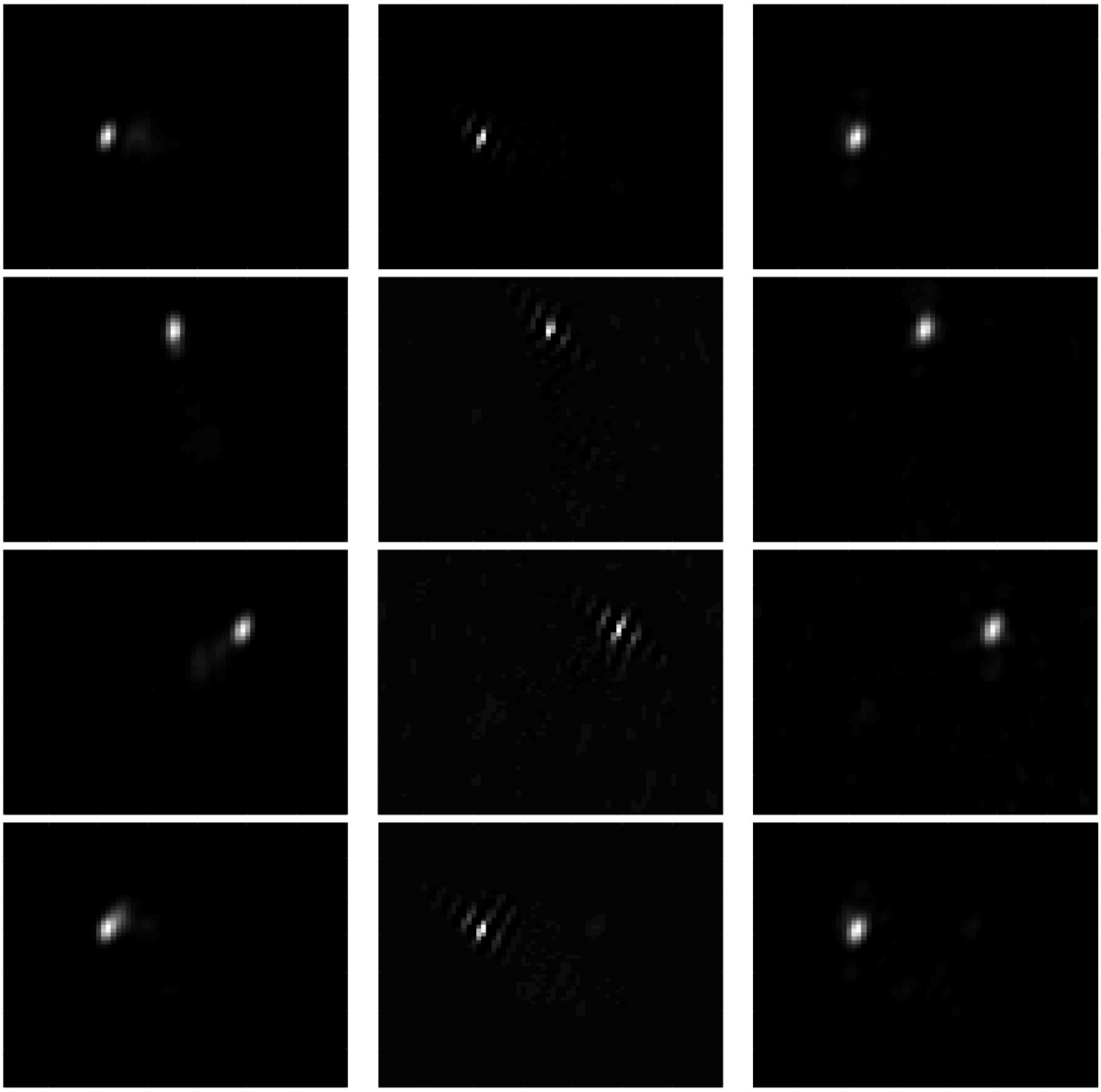

FIGURE 8. Continued reconstruction results of data 25 to 28. Left to right: ground truth image, TV, and proposed.

4. **Conclusions.** We have proposed a magnitude difference averaging, an additional method to improve the total variation (TV) performance. We utilize the magnitude difference TV result and ground truth signal in the training images. A similar pattern of the magnitude difference is also found in the testing image. This method's benefit suits some measurement applications with similar object structures. Therefore, in this paper, we applied this method to quasar images. In this study, we only have one sampling pattern. In case of different sampling patterns, we must train the images again. The images with specific sampling patterns of measurement cannot be reconstructed using different sampling patterns used in the training. We can only use the same sampling pattern in the training and testing. That is the limitation of this study.

Acknowledgment. This work is supported by Telkom University. The authors also gratefully acknowledge the helpful comments and suggestions of the reviewers, which have improved the presentation.

REFERENCES

[1] L. I. Rudin, S. Osher and E. Fatemi, Nonlinear total variation noise removal algorithm, *Physica D*, vol.60, pp.259-268, 1992.
[2] K. Bredies and M. Holler, Higher-order total variation approaches and generalisations, *Inverse Problems*, vol.36, no.12, DOI: 10.1088/1361-6420/ab8f80, 2020.
[3] Z. Du, D. Liu, G. Wu, J. Cai, X. Yu and G. Hu, A high-order total-variation regularisation method for full-waveform inversion, *Journal of Geophysics and Engineering*, vol.18, no.2, pp.1-12, 2021.
[4] M. Geng, L. Yang, Z. F. Pang and H. Zhu, Weighted-type image segmentation model via coupling heat kernel convolution with high-order total variation, *Journal of Nonlinear and Variational Analysis*, vol.7, no.4, pp.487-503, 2023.
[5] M. R. Chowdhury, J. Qin and Y. Lou, Non-blind and blind deconvolution under Poisson noise using fractional-order total variation, *Journal of Mathematical Imaging and Vision*, vol.62, no.8, 2020.
[6] L. Wu, L. Tang and C. Li, Hybrid regularization model combining overlapping group sparse second-order total variation and nonconvex total variation, *Journal of Electronic Imaging*, vol.31, no.4, 2022.
[7] T. Adam and R. Paramesran, Hybrid non-convex second-order total variation with applications to non-blind image deblurring, *Signal Image and Video Processing*, vol.14, no.1, pp.115-123, 2020.
[8] E. J. Candes, J. Romberg and T. Tao, Robust uncertainty principles: Exact signal reconstruction from highly incomplete frequency information, *IEEE Transactions on Information Theory*, vol.52, no.2, pp.489-509, 2006.
[9] *Large VLBA Project BEAM-ME (Successor to VLBA-BU-BLAZAR): Total & Polarized Intensity Images of Gamma-Ray Bright Blazars at 43 & 86 GHz*, https://www.bu.edu/blazars/BEAM-ME.html, 2023.
[10] D. E. Gary, *Radio Astronomy, Lecture #6: Fourier Synthesis Imaging*, https://web.njit.edu/∼gary/728/Lecture6.html, 2023.
[11] Z. Wang, A. C. Bovik, H. R. Sheikh and E. P. Simoncelli, Image quality assessment: From error visibility to structural similarity, *IEEE Transactions on Image Processing*, vol.13, no.4, 2004.

Author Biography

Ratri Dwi Atmaja received bachelor's and master's degrees in Telecommunications Engineering from Institut Teknologi Telkom (now Telkom University), Bandung, Indonesia in 2009 and 2011, respectively. He is currently a Lecturer in the School of Electrical Engineering at Telkom University. His research activities are in the topic of image and video signal processing.

Sugondo Hadiyoso received bachelor's and master's degrees in Telecommunications Engineering from Institut Teknologi Telkom (now Telkom University), Bandung, Indonesia in 2010 and 2012, respectively. He received Doctoral's degree in Electrical Engineering from Institut Teknologi Bandung, Bandung, Indonesia in 2023. From 2015 to 2018, he was a Head of the Telecommunications Technology Expertise Group at Telkom University. He has also been an Associate Professor/Lecturer of Faculty of Applied Science since 2010 and Head of the Telecommunications Technology Expertise Group from 2023 until now at Telkom University. His research interests and experiences include biomedical signal analysis, image and signal processing, and telecommunication technology.